# Measuring spike train synchrony

Thomas Kreuz,[1,*] Julie S. Haas,[2] Alice Morelli,[3] Henry D. I. Abarbanel,[2,4] and Antonio Politi[5]

[1]*Istituto dei Sistemi Complessi - CNR, Via Madonna del Piano 10, I-50019 Sesto Fiorentino, Italy*
[2]*Institute for Nonlinear Sciences, University of California, San Diego, USA*
[3]*Istituto Nazionale di Ottica Applicata, Firenze, Italy*
[4]*Department of Physics and Marine Physical Labaratory (Scripps Institution of Oceanography), University of California, San Diego, USA*
[5]*Istituto dei Sistemi Complessi - CNR, Sesto Fiorentino, Italy*

(Dated: January 24, 2007)

Estimating the degree of synchrony or reliability between two or more spike trains is a frequent task in both experimental and computational neuroscience. In recent years, many different methods have been proposed that typically compare the timing of spikes on a certain time scale to be fixed beforehand. Here, we propose the ISI-distance, a simple complementary approach that extracts information from the interspike intervals by evaluating the ratio of the instantaneous frequencies. The method is parameter free, time scale independent and easy to visualize as illustrated by an application to real neuronal spike trains obtained in vitro from rat slices. In a comparison with existing approaches on spike trains extracted from a simulated Hindemarsh-Rose network, the ISI-distance performs as well as the best time-scale-optimized measure based on spike timing.

Keywords: time series analysis; spike trains; event synchronization; reliability; clustering; neuronal coding

## I. INTRODUCTION

The basic elements of neuronal communication are pulsed electric signals called action potentials or spikes. Under the assumption that both the shape of the spike and the background activity carry minimal information, neuronal responses are typically reduced to the much simpler form of a spike train, where the only information maintained is the timing of the single spikes. Measuring the overall degree of synchrony between different spike trains is an important tool in many different contexts. It can be used to quantify the reliability of responses upon repeated presentations of the same stimulus [1], to address questions regarding the limitations of neuronal coding (rate versus time coding) [2] or to evaluate the information transfer between synaptically coupled neurons (cf., e.g., Ref. [3]).

A variety of different measures have been introduced to address the synchrony between spike trains. Most of these measures require considering a large number of trials, not just two. Some of them rely on the construction of a post-stimulus time histogram (PSTH), constructed from multiple trials. PSTH measures such as reliability, precision and sparseness [1, 4] rely on the analyst to define the so-called events, i.e., bursts of high firing frequency. Other methods (i) quantify the occurrence of given spike patterns and measure their robustness ("attractor reliability" [5]), (ii) exploit the deviation of the spike train statistics from a Poissonian distribution [6, 7], or (iii) measure the normalized variance of pooled exponentially convolved spike trains [8].

The focus of this study lies on a group of measures that aim at a quantification of the degree of similarity or dissimilarity between as few as two spike trains. A very prominent example of such bivariate approaches are spike train distances that consider spike trains to be points in an abstract metric space and assign non-negative values quantifying the dissimilarity between a given pair of spike trains. Among these is the distance introduced by Victor and Purpura [9], which evaluates the "cost" needed to transform one spike train into the other, using only certain elementary steps. Another metric proposed by van Rossum [10] measures the Euclidean distance between the two spike trains after convolution of the spikes with an exponential function. Other approaches quantify the cross correlation of spike trains after exponential or Gaussian filtering [11, 12], or exploit the exponentially weighted distance to the nearest neighbor [13]. A common property of all these measures is the existence of one parameter that sets the time scale for the analysis. This parameter does not exist for event synchronization, a method proposed by Quian Quiroga and colleagues [14], that quantifies the number of quasi-simultaneous appearances, using a variable time scale that automatically adapts itself to the local spike rates.

In this study a measure is proposed that, complementary to the approaches mentioned above, uses the interspike interval (ISI) instead of the spike as the basic element of comparison. The ISI-distance quantifies the ratio of instantaneous frequencies and facilitates visualization of the relative timing of pairs of spike trains. Since no binning is used, the measure has the maximum possible time resolution (i.e., up to a single spike). Similar to event synchronization, it is both parameter–free and self-adaptive so that there is no need to fix a time scale beforehand. In the first part of this study, the ISI-distance is illustrated using real in vitro data from cortical cells.

Moreover, since a comprehensive comparison of different approaches in a controlled setting was still missing,

*Electronic address: thomas.kreuz@fi.isc.cnr.it

we tested several bivariate measures of spike train synchrony (including the ISI-distance) on a large number of spike trains. These were generated from a network of simulated Hindemarsh-Rose neurons with a pre-determined degree of coupling between pairs. In this scenario, different spike trains belonged to different clusters and the capability of the measures to detect the original clustering behavior could be quantified by two indices, which evaluate the correctness of the clusters and the separation between them, respectively. In a final step, to assess the similarity of the different approaches to measure spike train synchrony, we evaluated the degree of redundance between the different measures by means of a correlation analysis.

The remainder of the paper is organized as follows: In the methods section, after a short description of the spike detection algorithm (Section II A), a more detailed description of the new method based on the ISI-distance is given (Section II B). It is illustrated using in vitro recordings from cortical cells in the entorhinal cortex of rats. The following section, II C, contains a short overview over the existing measures against which this new method is compared. The cluster analysis is described in Section II D, while the correlation analysis is described in section II E. In section III A the actual comparison of the different methods on simulated time series taken from a network of Hindemarsh-Rose model-neurons is carried out. Conclusions are drawn in section IV. Finally, both data sets (the in vitro recordings and the simulated Hindemarsh-Rose time series) are described in the appendix in sections A 1 and A 2, respectively.

## II. METHODS

### A. Spike detection

A prerequisite to any method is the extraction of the spike times from the time series by means of a standard spike detection algorithm. Typically, some sort of threshold criterion is employed, either for the time series itself or its derivative. Thereby the continuous time series is transformed into a discrete series of spikes. Each spike train can then be expressed as a series of $\delta$ functions

$$S(t) = \sum_{i=1}^{M} \delta(t - t_i) \tag{1}$$

with $t_1, ...t_M$ denoting the series of spike times and $M$ being the number of spikes.

In this study, for all the different measures the same spike detection algorithm is used. The threshold is chosen as the arithmetic average between the minimum and maximum value of the action potential.

### B. The ISI-distance

To obtain a time-resolved measure of the frequency of the spike train $\{t_i^x\}$, the value of the current interspike interval is assigned to each time instant [29],

$$x_{isi}(t) = \min(t_i^x | t_i^x > t) - \max(t_i^x | t_i^x < t) \quad t_1^x < t < t_M^x \tag{2}$$

Now, given a second spike train $\{t_j^y\}$, the ratio between $x_{isi}$ and $y_{isi}$ is taken (effectively, this is done just once after every new spike in either time series), and the final measure is thereby obtained after introducing a suitable normalization,

$$I(t) = \begin{cases} x_{isi}(t)/y_{isi}(t) - 1 & \text{if } \; x_{isi}(t) <= y_{isi}(t) \\ -(y_{isi}(t)/x_{isi}(t) - 1) & \text{else} \end{cases} \tag{3}$$

Accordingly, the measure becomes zero in case of isofrequent behavior, and approaches $-1$ and 1, respectively, if the spiking frequency of the first (or second) train is infinitely high and the other infinitely low.

In order to derive a measure of spike train distance, there are two possible ways of averaging. In the time-weighted variant, the absolute ISI-distance is integrated over time,

$$D_I = \int_{t=0}^{T} dt |I(t)|, \tag{4}$$

whereas in the spike-weighted variant, the ISI-distance is evaluated only after every new spike in either time series,

$$D_I^s = \sum_{i=1}^{M} |I(t_i)|. \tag{5}$$

All of these procedures can also be implemented by using a moving-window analysis. The advantage of this method is the self-adaptation to the shortest possible time-scale and thus can be implemented for rather short time series. On the other hand, in the case of a strong sensitivity to short time scales, one can easily obtain a coarse-grained evolution, by extending the definition to neighboring ISIs. An example of a possible application is the quantification of (dis-)similarities between bursts in time series.

In Fig. 1 the ISI-distance is applied to two exemplary input-output spike trains of 10 $s$ duration (for a description of the data see Appendix A 1). In the first seconds, the spike trains are 1 : 1 synchronized and this is reflected by an ISI-distance $I(t) \approx 0$. Nevertheless, small deviations can be visualized that are hard to catch from a visual inspection of the spike trains themselves. These deviations are more pronounced in the second half of the recording where the output no longer follows the input but rather slows down (as reflected by predominantly negative values marked in red) and a spike doublet occurs (as indicated by the short excursion to positive values

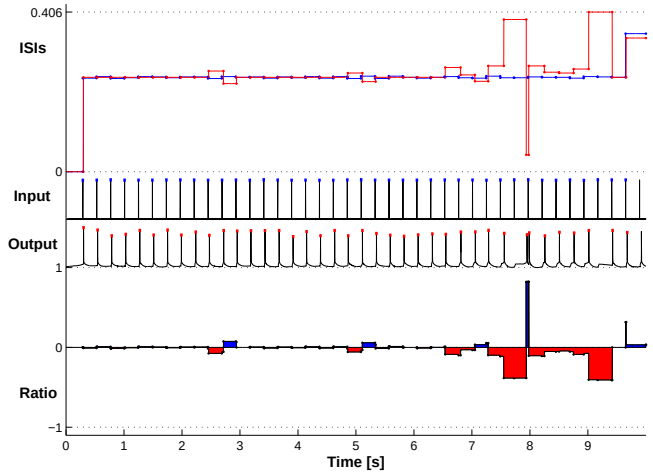


FIG. 1: First example of cortical cell recordings. In the middle traces the two recorded time series are shown. The detected spikes are marked in blue (input) and red (output), respectively. On top the ISI-values according to Eq. 2 are depicted, at the bottom the corresponding renormalized ISI-distance (cf. Eq. 4). Here colors mark the times where the respective spike train is slower. For this pair of spike trains an ISI-distance $D_I = 0.062$ is obtained.

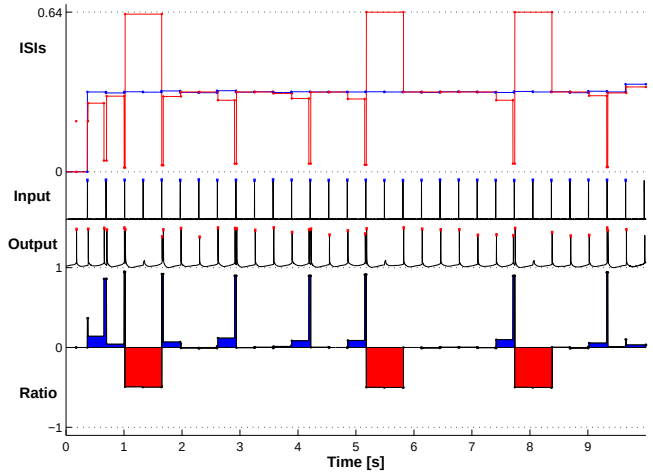


FIG. 2: Second example of cortical cell recording shown in the same way as in Fig. 1. In this case the ISI-distance attains the value $D_I = 0.15$.

marked in blue). The example shown in Fig. 2 reveals that certain patterns in the ISI-distance appear repeatedly. The output exhibits several spike doublets, some of which are followed by a miss (reflected by the negative values marked in red). Finally, a more irregular behavior is shown in Fig. 3 where it is again clear that the ISI-distance allows tracing the relative frequency behavior in a simple way.

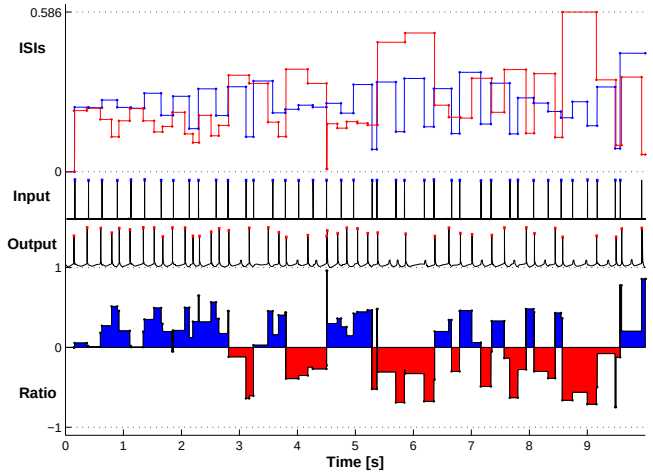


FIG. 3: Third example of cortical cell recording shown in the same way as in Fig. 1. The ISI-distance for this example is $D_I = 0.32$.

### C. Existing measures of spike train distance

In this study the ISI-distance will be compared against five existing measures of spike train (dis-)similarity. These comprise the spike train metrics introduced by Victor and Purpura [9] as well as by van Rossum [10], a correlation measure proposed by Schreiber and colleagues [12], another distance measure introduced by Hunter and Milton [13], and, finally, event synchronization, a method introduced by Quian Quiroga and colleagues [14].

In order to compare the various measures, we turned each of them into a suitably-normalized measure of dissimilarity, as the latter is more akin to the concept of distance.

#### 1. *Victor-Purpura spike train metric*

The spike train metric $D_V$ introduced in Ref. [9] defines the distance between two spike trains in terms of the minimum cost of transforming one spike train into the other by using just three basic operations: spike insertion, spike deletion and spike movement. While the cost of insertion or deletion of a spike is set to one, the cost $c_V$ of moving a spike is the only parameter of the method setting the time scale of the analysis. For small $c_V$, the distance basically equals the difference in spike number, whereas for high $c_V$, the distance approaches the number of non-coincident spikes, since instead of shifting spikes it becomes more favorable to delete all non-coincident spikes of the one time series and to insert all non-coincident spikes of the other. Thus, by increasing the cost $c_V$, the distance is transformed from a rate distance to a timing distance.

#### 2. Van Rossum spike train metric

A second spike train metric was introduced in Ref. [10]. In this method, each spike is convolved with an exponential function $e^{-(t-t_i)/\tau_R}$ $(t > t_i)$, where $t_i$ is the spike time. From the convolved waveforms $f(t)$ and $g(t)$, the van Rossum distance $D_R$ can be calculated as

$$D_R(\tau_R) = \frac{1}{\tau_R}\int_0^\infty [f(t) - g(t)]^2 dt \tag{6}$$

Since the post-synaptic currents triggered by the single spikes approximate exponentials, the van Rossum distance estimates the difference in the effect of the two trains on the respective synapses. In this method, the time constant $\tau_R$ of the exponential is the parameter setting the time scale. It is the inverse of Victor and Purpura's cost parameter: $\tau_R = 1/c_V$.

#### 3. Schreiber et al. similarity measure

The correlation-based approach was first described in Ref. [11], and later detailed in Ref. [12]. In this approach, each spike train is convolved with a filter of a certain width (exponential in [11], Gaussian in [12]) to form $s_i$ before cross correlation and normalization.

$$S_S(\sigma_S) = \frac{s_i s_j}{|s_i||s_j|}. \tag{7}$$

Haas and White allowed a minimal phase lag in the cross correlation (and thus another parameter to adjust), while Schreiber et al. allowed none. Here, the approach by Schreiber et al. is used. The width of the convolving filter $\sigma_S$ sets the time scale of interaction between the two spike trains. The inversion $D_S = 1 - S_S$ yields a normalized measure of spike train dissimilarity that can be compared with the other. A clustering analysis based on this measure was performed in Ref. [15].

#### 4. Hunter-Milton similarity measure

This approach, introduced in Ref. [13], starts by identifying in the spike train $y$ the nearest spike $t^y_{k(i)}$ to the spike occurring at time $t^x_i$ in the spike train $x$. The degree of coincidence between these spikes is quantified by $r_{xy} = \exp\left(-|t^x_i - t^y_{k(i)}|/\tau_H\right)$ and the overall similarity measure $S_H$ is thereby determined as the symmetrized average of$r_{xy}$ over the entire series,

$$S_H = \frac{\langle r_{xy}\rangle + \langle r_{yx}\rangle}{2}. \tag{8}$$

Also in this method, there is a free time scale that can be set by fixing the parameter $\tau_H$. For two identical spike trains $r_{xy} = r_{yx} = 1$. Accordingly, a measure of spike train dissimilarity can be obtained as $D_H = 1 - S_H$

#### 5. Event synchronization

The last measure is a variant of the event synchronization proposed in Ref. [14], and later used in Refs. [16, 17, 18]. This measure quantifies the overall level of synchronicity from the number of quasi-simultaneous appearances of spikes. However, in contrast to the measures introduced above, this method is scale-free, since the maximum time lag $\tau_{ij}$ up to which two spikes $t^x_i$ and $t^y_j$ are considered to be synchronous is adapted to the local spike rates according to

$$\tau_{ij} = \min\{t^x_{i+1} - t^x_i, t^x_i - t^x_{i-1}, t^y_{j+1} - t^y_j, t^y_j - t^y_{j-1}\}/2. \tag{9}$$

Then the function $c(x|y)$ is introduced to count the number of times a spike appears in $x$ shortly after a spike appears in $y$,

$$c(x|y) = \sum_{i=1}^{M_x}\sum_{j=1}^{M_y} J_{ij}, \tag{10}$$

where

$$J_{ij} = \begin{cases} 1 & \text{if } \ 0 < t^x_i - t^y_j \le \tau_{ij} \\ 1/2 & \text{if } \ t^x_i = t^y_j \\ 0 & \text{else} \end{cases} \tag{11}$$

With $c(y|x)$ defined accordingly, we can write the event synchronization as

$$Q = \frac{c(y|x) + c(x|y)}{\sqrt{M_x M_y}}. \tag{12}$$

Again, a measure of spike train distance can be defined as $D_Q = Q - 1$. With the above normalization, $0 \le D_Q \le 1$, with $D_Q = 0$ if and only if all spikes of the signals are synchronous [30].

### D. Assessing clustering quality

One important application for measures of spike train synchrony is the identification of interspike correlations and the reconstruction of clustering patterns. In order to test the above measures, we generated 29 spike trains by simulating a network of Hindmarsh-Rose neurons (see appendixA 2). From the network architecture and the pattern coding, we organized the 29 spike trains into three principal clusters with 13 members (clusters 1 and 2) and 3 members (cluster $S$), respectively. We first validated the different measures and then quantified their performance in reproducing the cluster structure by means of two indices. For the four measures $D_V$, $D_R$, $D_S$ and $D_H$ that depend on a parameter setting the time scale, we varied the respective parameter over several logarithmic decades, with four equidistant values within each decade, i.e., $c_V = 10^{-a+0.25b}$. In each case, we adapted the parameter range via $a$ and $b$ to cover the relevant extreme cases.

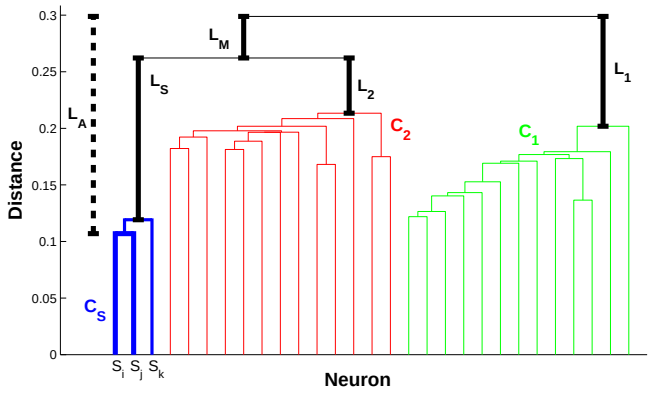


FIG. 4: Example of a hierarchical cluster tree obtained from 29 Hindemarsh-Rose time series employing the event distance $D_Q$. The three principal clusters $C_1$, $C_2$ and $C_S$ are distinguished by different colors. The merging of the first two time series $S_i$ and $S_j$ to cluster $C_\alpha$ is highlighted by very thick blue lines, the consecutive merging of this cluster with $S_k$ by thick blue lines. Finally, black lines mark the separation of the three principal clusters used for the definition of the cluster-separation $F$. The clustering performance values for this example are $H = 1$ and $F = 0.57$.

After applying a given similarity measure to all possible pairs of spike trains, we generated a hierarchical cluster tree (dendrogram) by applying the single linkage algorithm provided by Matlab to the resulting pairwise distance matrices. An exemplary dendrogram obtained from the 29 Hindemarsh-Rose time series using the event distance $D_Q$ is shown in Fig. 4. Three principal clusters are clearly distinguished. The dendrogram is constructed as follows: First, the closest pair $S_i$, $S_j$ of sequences is identified and thereby linked by a $\sqcap$-shaped line, where the height of the connection measures the mutual distance $d(S_i, S_j)$. These two time series are merged into a single element $C_\alpha$, and the next closest pair of elements is then identified and connected. The procedure is repeated iteratively until a single cluster remains. The implementation of the method requires introducing the distance between a pair of clusters $C_\alpha$, $C_\beta$. In the single linkage algorithm, it is defined as the minimum over all the distances between pairs of sequences in the two clusters, i.e., $d(C_\alpha, C_\beta) = \min\{d(S_k, S_m)\}$, $S_k \in C_\alpha$, $S_m \in C_\beta$.

In order to quantify the success in reproducing this clustering, we computed the entropy of the confusion matrix $N_{\alpha\beta}$) [9, 19]. The entry $N_{\alpha\beta}$ is defined as the number of times $S_\beta$ is the closest cluster to a spike train belonging to $S_\alpha$. Following Ref. [9], the distance between the spike train $S_i$ and the cluster $C_\alpha$ is defined as $\langle d(S_i, S_j)\rangle_\alpha$, where $\langle\cdot\rangle_j$ denotes the average of all spike trains in the cluster $C_\alpha$. Note that this distance is different from the one used for the cluster identification, however, we verified that results proved to be robust against variations of the distance used. For a perfect clustering $N$ is diagonal, whereas each misclassification yields a non-diagonal elements. The relative amount of misclassifications is finally quantified by the entropy

$$H_C = \sum_{\alpha,\beta} p_{\alpha\beta} \log \frac{p_{\alpha\beta}}{P_\alpha Q_\beta} \tag{13}$$

where $p_{\alpha\beta} = N_{\alpha\beta}/N_{tot}$, $P_\alpha = \sum_b p_{\alpha b}$, and $Q_\beta = \sum_b p_{b\beta}$. This entropy value is then normalized to the maximum entropy obtained for a correct classification [31],

$$H = H_C/H_{max}. \tag{14}$$

Although the clustering entropy $H$ evaluates the correctness of the hierarchical tree, it does not quantify the separation of the three principal clusters in those cases where the expected clustering is obtained. As can be seen in Fig. 4, the cluster separation is given by the lengths $L_1$, $L_2$, $L_S$, and $L_M$ of their upper branches. A convenient way of quantifying the cluster separation with a single indicator is by introducing the index

$$F = \frac{L_1 + L_2 + L_S + L_M}{3L_A}, \tag{15}$$

where the branch lengths are normalized to the difference $L_A$ between the overall maximum and the overall minimum distance thus guaranteeing that the $F$-values range in the interval $[0, 1]$. Given a correct clustering with three principal clusters, all quantities needed for the calculation of $F$ can be extracted from the output matrix of the Matlab single linkage algorithm, otherwise the clustering separation is set to $F = 0$.

### E. Correlations between the different measures

In order to investigate to which extent the different measures of spike train distance carry independent and non-redundant information, we performed a correlation analysis. First, for each of the four measures $D_V$, $D_R$, $D_S$, and $D_H$ that depend on a parameter setting the time scale, we identified the parameter value yielding the best clustering results. Then, we applied each of the six measures ($D_I$, $D_V$, $D_R$, $D_S$, $D_H$, and $D_Q$) to the different pairs of sequences, obtaining six sets of $29 \times 28/2 = 406$ different values. In order to guarantee maximal homogeneity, the various measures were all scaled to the $[0, 1]$ range (this means that the two unnormalized measures $D_V$ and $D_R$ were divided by their maximal values). Moreover, following a customary approach, each data set was arcsin-transformed to better fit a normal distribution [20]. Finally, we determined the Pearson correlation coefficients [21] and from the pairwise distances (1-correlation) among the different measures we obtained a hierarchical cluster tree (using again the single-linkage algorithm).

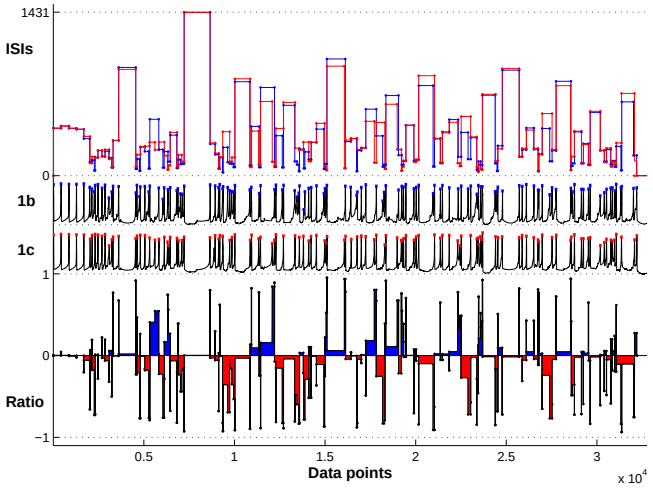


FIG. 5: Two time series from two neurons coding both for the same pattern B (middle). The detected spikes are marked in blue and red, respectively. On top the ISIs, at the bottom the corresponding renormalized ISI-distance. Here colors mark the times where the respective spike train is slower. For this combination an ISI-distance $D_I = 0.019$ is obtained.

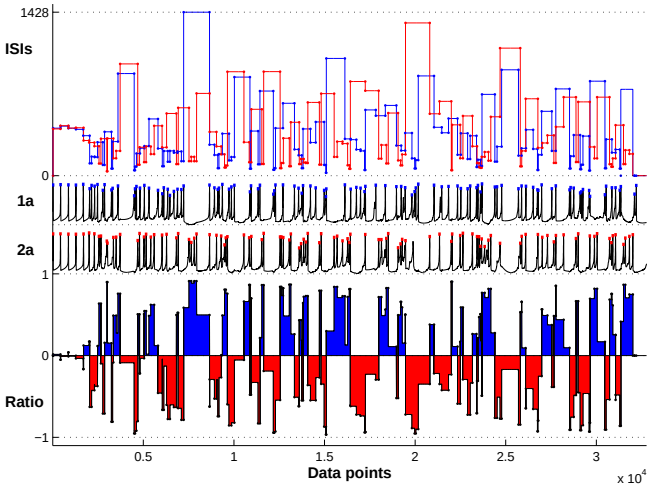


FIG. 6: Same as Fig. 5 but this time for two time series from two neurons coding for different patterns. In this case the ISI-distance $D_I = 0.032$ is much higher.

## III. RESULTS

### A. Comparison of measures using simulated Hindemarsh-Rose time series

In order to compare the various dissimilarity measures, we have analyzed also numerically generated spike trains, since their properties are much more controllable. More precisely, we refer to Hindemarsh-Rose time series whose clustering properties are known beforehand (see appendixA 2 for a description of the underlying model). Two instances of the ISI-distance are shown in Figs. 5 and 6 where the signals emitted by two neurons belonging to the same and to different clusters, respectively, are compared. In the first example, deviations from zero of the ISI-distance are confined to short time scales (they are mostly due to small phase shifts that accompany large changes of the spiking-frequency). In the second example, long-lasting differences are detected which also exhibit a sort of oscillation.

The distance matrix obtained from the application of the ISI-distance $D_I$ to all 406 combinations of the 29 spike trains is shown in Fig. 7. Patterns can be clearly recognized, since the neurons have been ordered according to to their a priori affiliation known from the model setup. Smallest distances are obtained for pairs of spike trains belonging to the same cluster starting from those within $S$. At the other extreme, the largest distances are found for spike trains belonging to the clusters 1 and 2.

From this distance matrix, we generated the cluster dendrogram shown in Fig. 8, where the three principal clusters are clearly visible. The absence of misclassifications implies that the clustering entropy (computed according to Eqs. (13,14)) is $H = 1$. On the other hand,

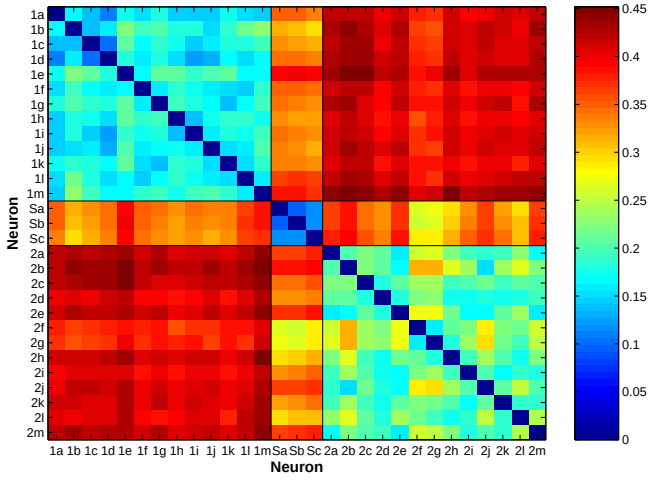


FIG. 7: Distance matrix for 29 time series from the Hindemarsh-Rose model. Results are obtained by using the ISI-distance $D_I$. Neurons are labelled by '1', '2' and 'S', respectively, depending on their affiliation to pattern 1, 2 or both ('shared').

the cluster separation determined from Eq. (15) is for this case $F = 0.66$. Similar results have been obtained for the other parameter-free measure, the event distance $D_Q$ (the corresponding dendrogram being shown in Fig. 4). Also in this case, $H = 1$, while the smaller value of $F$ (0.60) suggests a slightly lower clustering quality.

We then investigated the performance of the Victor-Purpura and van Rossum spike train distances, as well as of the Schreiber et al. and Hunter-Milton dissimilarities for different values of the free parameter in order to select the proper time scale. In Fig. 9 the Victor-Purpura spike train distance $D_V$ is plotted against the cost parameter $c_V$ for all pairs of spike trains in a group containing three members in each of the three principal clusters. The relative order of the six different combina-

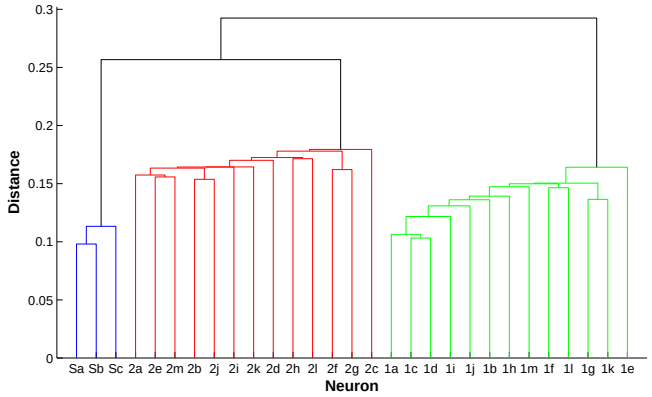


FIG. 8: Clustering of 29 time series from the Hindemarsh-Rose model using the ISI-distance. The existence of three clearly separated clusters is evident. The cluster performance values are $H = 1$ and $F = 0.66$.

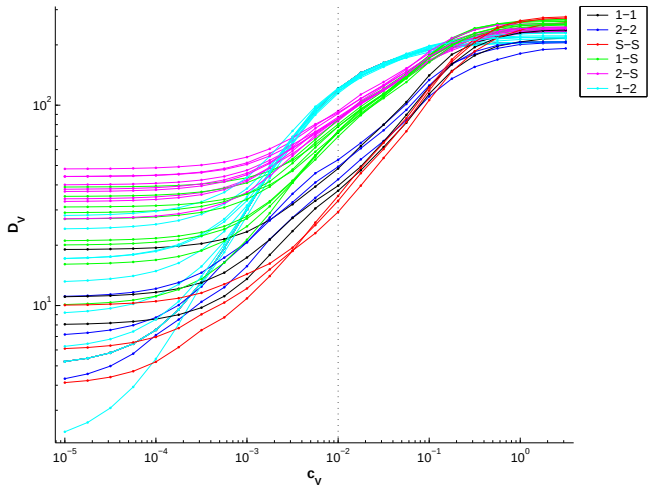


FIG. 9: Dependence of the Victor-Purpura spike train distance $D_V$ on the cost parameter $c_V$. For each combination of cluster affiliations a different color is used. The dotted line marks the cost value for which the best clustering separation is obtained.

tions of cluster affiliations ($1-1$, $1-2$, $1-S$, $2-2$, $2-S$, $S-S$) depends on the cost parameter. At small $c_V$ values, the Victor-Purpura distance measures the difference in spike counts and this number seems not to be closely related to the type of underlying cluster (see in particular the spread of the $D_V$-values corresponding to the $1-2$ combination). At high $c_V$ values, distances are larger and also very mixed. It is only at intermediate values that a clear separation of the six different cluster combinations can be observed. High values are obtained for all the $1-2$ combinations while the intra-cluster $S-S$ distance is the smallest one.

We find similar results for the other parameter–dependent measures. In all cases, there exists an intermediate parameter range where meaningful results can be obtained (i.e. the cluster entropy is equal to 1), while for higher and lower values no clear clustering can be

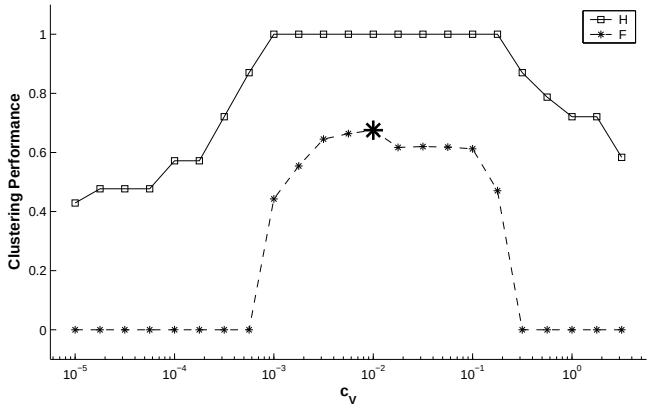


FIG. 10: For the Victor-Purpura spike train distance the clustering entropy $H$ (solid line) and the cluster separation $F$ (dashed line) in dependence of the parameter $c_V$ that sets the time scale. Remember that $F$ is only calculated for those cases where a correct clustering (as reflected by $H = 1$) is obtained. The optimum performance $F = 0.68$ is marked by a large asterisk at $c_V = 0.01$.

recognized. The role of the free parameter is better seen by determining the clustering performance for different values of the parameter itself. In Fig. 10, the two indices $H$ and $F$ are plotted for the Victor-Purpura distance $D_V$ versus the cost parameter $c_V$. We see that a perfect clustering is found only inside an intermediate range, where $H = 1$; the smaller $H$ values found outside this interval reflect the presence of misclassifications in the clustering tree. Inside the interval where the right classification is obtained, we computed the clustering separation $F$. This index attains its peak value $F = 0.68$ when $c_V = 0.01$, which we thus identify as the optimal value of the time-scale for the separation the different clusters. This result is consistent with the visual impression when looking at Fig. 9 (the vertical line corresponds to the optimal $c_V$ value). A similar scenario is found also for the other measures that depend on a time scale. In each case there exists an intermediate range where $H = 1$. The broadest range is found for the Victor-Purpura and the van Rossum distance.

The performance of the different measures are compared in Fig. 11, where the maximum value of the cluster separation is shown for each spike train distance (for the parameter-free ISI-distance and the event distance no optimization is required). The best results are found for the Victor-Purpura distance $D_V$, but the ISI-distance $D_I$ and the van Rossum distance $D_R$ perform almost equally well. At the other extreme, the poorest cluster separation is obtained for the Hunter-Milton dissimilarity $D_H$.

### B. Correlations between the different measures

In order to assess the degree of redundancy among the different measures of spike train dissimilarity, a correlation and cluster analysis has been performed on all 406

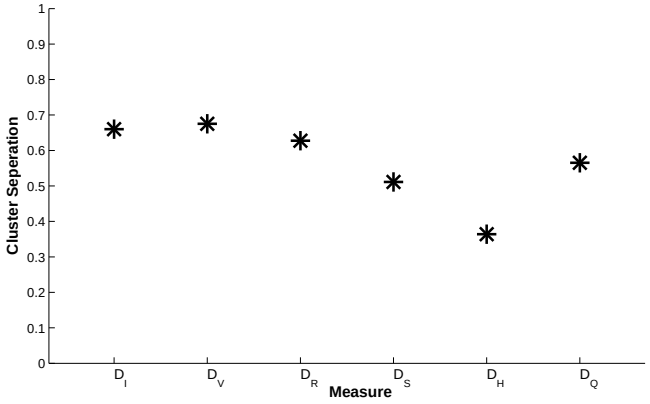


FIG. 11: Comparison of Measures: Separation of clusters.

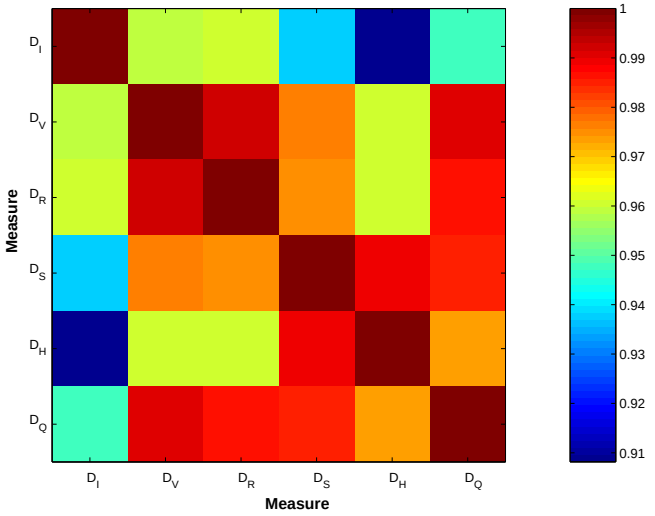


FIG. 12: Correlation coefficients between the six measures of spike train dissimilarity.

bivariate combinations of measure results by following the approach discussed in the previous section. Since the number of independent observations can hardly be estimated, this is only a relative examination. For this reason no values of significance are given.

As we see from the high overall level of correlation shown in Fig. 12, all measures seem to carry similar information. The minimum correlation coefficient 0.91 is obtained between the ISI-distance and the Hunter-Milton dissimilarity, while the spike train distances by Victor-Purpura and van Rossum appeared to be the most correlated measures. From the corresponding cluster tree (cf. Fig. 13), it becomes evident that the ISI-distance is the most independent measure, whereas the other measures belong to one big cluster. This reflects the fact that the ISI-distance is derived from interspike intervals, while the other measures are based on spike times.

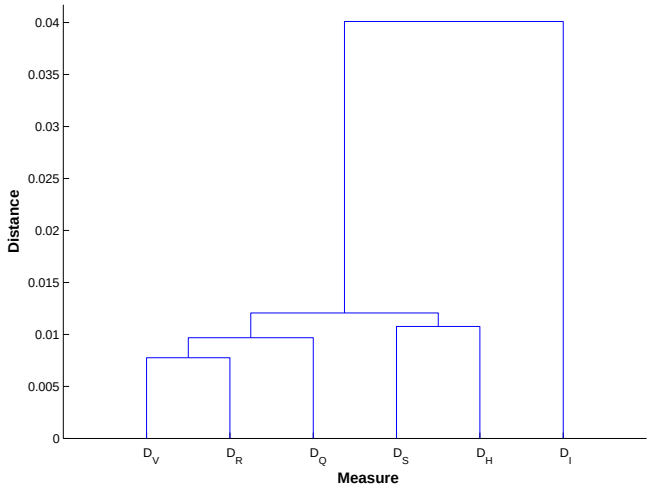


FIG. 13: Clustering for the six measures of spike train dissimilarity.

## IV. DISCUSSION

In this study we propose a simple method for measuring the (dis-)similarity of two spike trains. As an estimator based on the relative sizes of interspike intervals, the ISI-distance is complementary to all spike-based measures of synchrony that quantify the simultaneous occurrences of spikes via some sort of coincidence detection. As illustrated by an application to in vitro recordings of cortical cells, the measure serves also as an excellent means to visualize the occurrence of spiking pattern in the respective spike trains.

In order to judge the relative merit of the different methods, we compared the methods by evaluating each of them on spike trains extracted from a network of simulated Hindemarsh-Rose neurons. We assessed the ability of the different measures to reproduce the original clustering (established by a priori adjusting the synaptic couplings in the model) by means of two indices. In this comparison, no measure fails in reproducing the expected clustering, however, we found subtle differences in the degree of separation among the three clusters. The ISI-distance performed as well as the best spike-based measure (the Victor-Purpura distance $D_V$) with the advantage of not requiring the optimization of any parameter. In fact, the ISI-distance, like event synchronization, is self-adaptive in that it automatically identifies the proper time scale.

Finally, we implemented a correlation analysis in order to evaluate the degree of independence among the six different measures of spike train similarity. Since the overall level of correlation is quite high, all measures apparently access similar information. The subsequent cluster analysis reveals that the ISI-distance is the most independent approach. This is not surprising since the ISI-distance is the only measure that can be regarded as a measure of rate coding (since it is built on instantaneous frequency

estimates) whereas all other measures (that are based on spike timing) can be interpreted as measures of time coding.

Some general remarks concerning the application of measures of spike train (dis-)similarity: First, although the focus of this study is on the estimation of similarity between just two spike trains, all methods can also be used within a multivariate context. For example, in order to assess the reproducibility of neural spike train responses to an identical stimulus across many different presentations (trials), reliability can be defined as the average over all pairwise correlation-values (as done in Refs. [11, 12, 13]). On the other hand, it should be noted that the ISI-distance, like all the other measures, can be fooled by phase lags, no matter whether these are caused by internal delay loops in one spike train or by a common driver that forces the two time series with different delays. Thus any such phase lags should be removed by suitably shifting the time series before computing the measures.

The comparisons carried out in this study constitute an important step towards the identification of the most appropriate spike train (dis-)similarity for an application to real data. From the observed performance values and the results of the correlation analysis, we conclude that the ISI-distance together with either one of the spike based measures, such as the Victor-Purpura or the van Rossum spike train distance, or event synchronization is the most appropriate choice. However, it should also be noted that other possible criteria for the selection of an appropriate measure, such as computational cost or robustness against noise, remain to be evaluated in future studies.

## APPENDIX A: DATA

### 1. Application to in vitro recordings of cortical cells

The ISI-distance is illustrated using in vitro whole-cell recordings taken from cortical cells from the layer 2 medial entorhinal cortex of young Long-Evans rats. In these experiments (conducted as approved by the UCSD IACUC) cortical cells were selected from a slice preparation (400 micron) by their superficial position, as well as particular characteristics of their electrophysiological responses to long current steps (cf. Ref. [11]). Intracellular signals were amplified, low pass filtered, and digitized at 10 kHz via software created in LabView (National Instruments). Inputs were delivered as synaptic conductances through a linux-based dynamic clamp [22]. Inputs were comprised of synaptic inputs added to an underlying DC depolarization. The amplitude of the DC depolarization was tailored for each cell to elicit a spike rate of $5-10$ Hz. Synaptic inputs were of the form $Isyn = G_{syn}S(V_m - V_{syn})$ where $S$ follows the differential expression $dS/dt = \alpha(1-S) = \beta S$; $\alpha = 500/ms$, $\beta = 250/ms$, $V_{syn} = 0mV$. $G_{syn}$ was tailored for each cell to be peri-threshold and elicit a spike with probability between 50 and 100%. Synaptic events were delivered for 10 seconds at either regular intervals or chaotic intervals; the latter intervals were taken from a set of five 60 second recordings of SC spike times in response to steady DC depolarization alone.

### 2. Hindemarsh-Rose simulations

The spike trains have been generated using time series extracted from a larger network of Hindemarsh-Rose (HR) model-neurons [23] in the chaotic regime. This network was originally designed to analyze semantic memory representations using feature-based models; details of the network architecture and the implementation of the feature coding can be found in Ref. [24].

In short, the state the neuron $i$ is determined by three first-order differential equations describing the evolution of the membrane potential $X_i$, the recovery variable $Y_i$, and a slow adaptation current $Z_i$,

$$\dot{X}_i = Y_i - X_i^3 + 3X_i^2 - Z_i + I_i + \alpha_i(t) - \beta_i(t) \quad \text{(A1)}$$

$$\dot{Y}_i = 1 - 5X_i^2 - Y_i \quad \text{(A2)}$$

$$\dot{Z}_i = 0.006[4(X_i - 1.6) - Z_i], \quad \text{(A3)}$$

where

$$\alpha_i(t) = \sum_{j=1}^{\widehat{F}(\widehat{M}-1)} w_{ij}A_j(t) \quad \text{(A4)}$$

and

$$\beta_i(t) = \frac{1}{\widehat{F}-1}\sum_{k=1}^{\widehat{F}-1} A_k^{(i)}(t). \quad \text{(A5)}$$

The network consisted of $\widehat{N} = 128$ HR neurons belonging to $\widehat{M} = 16$ different modules with $\widehat{F} = 8$ neurons each. In a learning stage, input memory patterns were stored by updating the synaptic connection weights $w_{ij}$ between different neurons using a Hebbian mechanism based on the activity variables $A_j$. During the retrieval stage in which the learned connection weights were kept constant, the 29 time series to be analyzed were extracted. According to their coding properties regarding the retrieval of two distinguished memory patterns, the 29 time series belonged to three principal clusters, 13 of the corresponding neurons coded for pattern 1 only, 13 coded for pattern 2 only and 3 coded for both patterns (shared). The respective time series were labelled by '1', '2' and 'S' followed by an index letter. The numerical integration was done by using a fixed-step fourth-order Runge-Kutta method. The integration step-size was chosen equal to 0.05 ms of real time. The length of the time series analyzed was 32768 data points.

**Acknowledgements** We thank S. Luccioli, A. Torcini and K. Ulbrich for useful discussions and P. Grassberger for carefully reading this manuscript. TK has been supported by the Marie Curie Individual Intra-European Fellowship "DEAN", project No 011434. JSH acknowledges financial support by the San Diego Foundation.

[1] Mainen, Z., Sejnowski, T. J., 1995. Reliability of spike timing in neocortical neurons. Science 268, 1503.
[2] Rieke, F., Warland, D., de Ruyter van Steveninck, R., Bialek, W., 1996. Spikes: Exploring the neural code. Institute of Technology, Cambridge, Massachusetts.
[3] Reyes, A. D., 2003. Synchrony-dependent propagation of firing rate in iteratively constructed networks in vitro. Nature Neurosci 6, 593.
[4] Berry, M. J., Warland, D. K., Meister, M., 1997. The structure and precision of retinal spike trains. Proc. Natl. Acad. Sci. USA 94, 5411.
[5] Tiesinga, P. H. E., Fellous, J. M., Sejnowski, T. J., 2002. Attractor reliability reveals deterministic structure in neuronal spike trains. Neural Comput. 14, 1629.
[6] Brenner, N., Strong, S. P., Koberle, R., Bialek, W., de Ruyter van Steveninck, R. R., 2000. Synergy in a neural code. Neural Comput 12, 1531.
[7] Tiesinga, P. H. E., 2004. Chaos-induced modulation of reliability boosts output firing rate in downstream cortical areas. Phys. Rev. E 69, 031912.
[8] Hunter, J. D., Milton, G., Thomas, P. J., Cowan, J. D., 1998. Resonance effect for neural spike time reliability. J Neurophysiol 80, 1427.
[9] Victor, J., Purpura, K., 1996. Nature and precision of temporal coding in visual cortex: A metric-space analysis. J Neurophysiol 76, 1310.
[10] van Rossum, M. C. W., 2001. A novel spike distance. Neural Computation 13, 751.
[11] Haas, J. S., White, J. A., 2002. Frequency selectivity of layer II stellate cells in the medial entorhinal cortex. J. Neurophysiol. 88, 2422.
[12] Schreiber, S., Fellous, J. M., Whitmer, J. H., Tiesinga, P. H. E., Sejnowski, T. J., 2003. A new correlation-based measure of spike timing reliability. Neurocomputing 52, 925.
[13] Hunter, J. D., Milton, G., 2003. Amplitude and frequency dependence of spike timing: implications for dynamic regulation. J Neurophysiol 90, 387.
[14] Quian Quiroga, R., Kreuz, T., Grassberger, P., 2002. Event synchronization: A simple and fast method to measure synchronicity and time delay patterns. Phys. Rev. E 66, 041904.
[15] Fellous, J. M., , Tiesinga, P. H. E., Thomas, P. J., Sejnowski, T. J., 2004. Discovering spike patterns in neuronal responses. J Neurosci 24, 2989.
[16] Hahnloser, R. H. R., Kozhevnikov, A. A., Fee, M. S., 2002. An ultra-sparse code underlies the generation of neural sequences in a songbird. Nature 419, 65.
[17] Kreuz, T., Andrzejak, R. G., Mormann, F., Kraskov, A., Stögbauer, H., Elger, C. E., Lehnertz, K., Grassberger, P., 2004. Measure profile surrogates: A method to validate the performance of epileptic seizure prediction algorithms. Phys. Rev. E 69, 061915.
[18] Kreuz, T., Kraskov, A., Andrzejak, R. G., Mormann, F., Lehnertz, K., Grassberger, P., 2007. Measuring synchronization in coupled model systems: A comparison of different approaches. Phys D 225, 29.
[19] Abramson, N., 1963. Information theory and coding. McGraw-Hill, New York.
[20] Daniels, H. E., Kendall, M. G., 1947. The significance of rank correlation where parental correlation exists. Biometrika 34, 197.
[21] Devore, J., Peck, R., 2005. Statistics: The exploration and analysis of data. Duxbury Press, Belmont, CA.
[22] Dorval, A. D., Christini, D. J., White, J. A., 2001. Real-time linux dynamic clamp: A fast and flexible way to construct virtual ion channels in living cells. Annals of Biomedical Engineering 29, 897.
[23] Hindmarsh, J. L., Rose, R. M., 1984. A model of neuronal bursting using three coupled first order differential equations. Proc. R. Soc. London B 221, 87.
[24] Morelli, A., Grotto, R. L., Arecchi, F. T., 2006. Neural coding for the retrieval of multiple memory patterns. Biosystems 86, 100.
[25] Callenbach, L., Hänggi, P., Linz, S. J., Freund, J. A., Schimansky-Geier, L., 2002. Oscillatory systems driven by noise: frequency and phase synchronization. Phys. Rev. E 65, 051110.
[26] Freund, J. A., Schimansky-Geier, L., Hänggi, P., 2003. Frequency and phase synchronization in stochastic systems. Chaos 13, 225.
[27] Tiesinga, P. H. E., Sejnowski, T. J., 2004. Rapid temporal modulation of synchrony by competition in cortical interneuron networks. Neural Comput. 16, 251.
[28] Aronov, D., Reich, D. S., Mechler, F., Victor, J. D., 2003. Neural coding of spatial phase in V1 of the macaque monkey. J Neurophysiol 89, 3304.
[29] This is closely related to the Rice phase, that is obtained by linear interpolation between two events (e.g., spikes) from zero to $2\pi$ (cf., e.g., Refs. [25, 26]). In fact, the measure $I$ is proportional to the ratio of instantaneous Rice frequencies, however, the normalization used here allows for a better visualization.
[30] This normalization is superior to the normalization proposed for a similar measure in Ref. [27]. There, the so called coincidence factor was normalized to the minimum number of spikes in either spike train. With that normalization it would, in the extreme case, be possible that a single spike can synchronize perfectly with a very long spike train just because it coincides (maybe by chance) with one of the spikes in the other sequence. On the other hand, with the normalization used here, the maximum value can only be achieved for truly synchronous spike trains, whereas a difference in spike number is already correctly reflected by lower $Q$ values which indeed indicate a deviation from perfect synchrony. As an additional confirmation, we also find that the clustering performance is superior for the normalization proposed here (results not shown).
[31] The bias correction introduced in Ref. [28] is omitted since it is not necessary for a relative comparison of measures.